

Rare earth element geochemistry and strontium isotopic composition of a massif-type anorthositic–charnockitic body: the Hydra Massif (Rogaland, SW Norway)

DANIEL DEMAIFFE

Minéralogie-Pétrologie, Université Libre de Bruxelles, B-1050 Bruxelles, Belgium

and

JAN HERTOGEN*

Instituut voor Nucleaire Wetenschappen, Rijksuniversiteit Gent, B-9000 Gent, Belgium

(Received 12 August 1980; accepted in revised form 23 April 1981)

Abstract—The Hydra Massif (Rogaland Complex, SW Norway) mainly consists of plagioclase cumulates (anorthosites and leuconorites), which grade progressively into a fine-grained (200 μm), locally porphyritic, jotunitic rock towards the contact with the granulite facies gneisses. The massif is cross-cut by thin (10 cm up to 1 m) charnockitic dykes.

The petrographical and geochemical evolution of the Hydra Massif can be explained by fractional crystallization of a jotunitic parental magma. Major and trace element constraints indicate that mafic phases are underabundant in the exposed levels of the massif, most likely as a result of plagioclase flotation in the early stages of solidification. Partitioning into the cumulate minerals (mainly plagioclase and orthopyroxene) governs the trace element contents of the leuconoritic adcumulates. However, the trace element geochemistry of the apparently early formed anorthositic orthocumulates largely depends upon the amount of a trapped intercumulus liquid. On the basis of trace element abundances (high REE, Rb, Th, U; negative Eu anomalies) the silicic charnockitic dykes can be considered as the residual liquid of the anorthositic fractionation trend. The higher initial $^{87}\text{Sr}/^{86}\text{Sr}$ ratios (0.7086 ± 0.0006 vs 0.7055 ± 0.0004 for the plagioclase cumulates and jotunitites) point to contamination of the charnockitic liquids by surrounding gneissic material.

INTRODUCTION

THE ORIGIN of massif-type or Adirondack-type anorthosites (ANDERSON and MORIN, 1969) is one of the most debated problems of igneous petrology (e.g. CARMICHAEL *et al.*, 1974). The more important questions are the nature and origin of the parental magma of the anorthosite suite and the relationship between the anorthosites and the spatially related silicic rocks, mainly of charnockitic type (EMSLIE, 1978).

On the basis of geological and geophysical data, BUDDINGTON (1969) postulated that the anorthositic series derived from a liquid of gabbroic anorthositic composition. Such highly feldspathic parental magmas have also been proposed on the basis of trace element geochemistry, mainly of the REE (SIMMONS and HANSON, 1978; WIEBE, 1980; ASHWAL and SEIFERT, 1980). These authors do not favor a comagmatic character of charnockites and anorthosites. On the contrary, PHILPOTTS (1969) and DE WAARD *et al.* (1974) suggested, mainly on the basis of field relations, that charnockitic rocks appear to belong to the anorthositic differentiation sequence in some anorthositic massifs. Consequently, the parental magma should have an intermediate composition (monzodiorite–jotunitite). This view found some support in the

REE geochemistry of jotunitites from South Norway (DUCHESNE *et al.*, 1974).

This paper deals with the strontium isotopic composition and the REE geochemistry of the Hydra Massif, a small anorthositic–charnockitic body in the eastern part of the South Rogaland anorthositic–noritic–mangeritic Complex, SW Norway (P. MICHOT, 1960; J. MICHOT and P. MICHOT, 1969; DE WAARD *et al.*, 1974). The South Rogaland Complex is intruded in granulite facies gneisses of Sveconorwegian age (PASTEELS and MICHOT, 1975); U–Pb dating showed that the whole magmatic activity in the eastern part of the Complex was confined to a short time interval (955–910 Ma; PASTEELS *et al.*, 1979). Some geochemical aspects of jotunitites and charnockites from the South Rogaland Province have already been discussed in previous papers (DUCHESNE *et al.*, 1974; DUCHESNE and DEMAIFFE, 1978; DEMAIFFE *et al.*, 1979; DEMAIFFE and JAVOY, 1980; PETERSEN, 1980). We will present a semi-quantitative fractional crystallization model that accounts for most of the trace element variation trends in the Hydra jotunitite–anorthosite–leuconorite–charnockite series.

GEOLOGY AND PETROGRAPHY OF THE HIDRA ANORTHOSITIC–CHARNOCKITIC BODY

The field relations of the Hydra massif (Fig. 1a) with the other anorthositic masses and the granulite facies gneisses,

* Present address: University of Leuven, Fysico-chemische geologie, Celestijnenlaan 200C, B-3030 Leuven, Belgium.

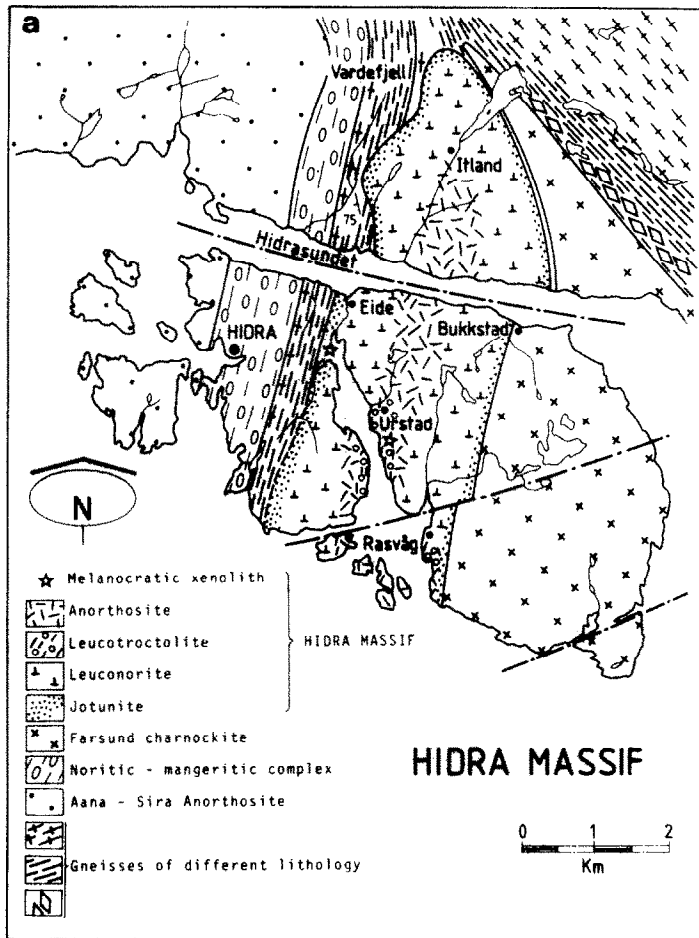


Fig. 1a. Geological sketch map of the Hidra Massif, a sub-unit of the Rogaland Complex, S.W. Norway.

and the general petrography of the different rocks units have been discussed by DEMAÏFFE *et al.* (1973) and DEMAÏFFE (1977b). The salient features are summarized below for easy reference.

It is important to note at the onset that the Hidra rocks have not been metamorphosed and that the original mineralogy has been well preserved. The lack of any deformation features indicates that the Hidra body has been emplaced after the major tectonic events that affected the gneissic envelope.

The main part of the Hidra massif is made up of a medium grained (1–3 cm) leuconorite (= gabbroic anorthosite) with a subophitic texture. The automorphic plagioclase is a calcic andesine (An_{43} – An_{49}), the orthopyroxene (En_{60} – En_{66}) is rich in Schiller inclusions, and the Fe-Ti oxides (fine hemoilmenite and homogeneous magnetite) have a poikilitic interstitial texture. Automorphic apatite crystals appear in the oxides. The leuconorite contains giant (up to 1 m) plagioclase megacrysts ($46 \pm 3\% An$).

Towards the center of the massif, the leuconorite grades into a true, coarse-grained anorthosite with well developed orthocumulate textures (DEMAÏFFE *et al.*, 1973): zonation of the cumulus plagioclase crystals, presence of interstitial K-feldspar and fine-grained quartz–K-feldspar micropegmatitic intergrowths (Fig. 2). This implies that part of the magmatic liquid has been trapped by the cumulus plagioclases.

A few meter-sized melanocratic pyroxenitic enclaves have been observed. They occur mainly in the leuconorite and predominantly consist of orthopyroxene laths. The orthopyroxene shows igneous lamination and is sur-

rounded by interstitial Fe-Ti oxides. Brown amphiboles, occurring as thin rims around the orthopyroxenes and the oxides are presumably of secondary or late stage origin.

The massif is cross-cut by charnockitic dykes and granitic pegmatitic lenses. They are intimately related to the anorthositic-leuconoritic rocks, but do not show any apparent relationship with the metamorphic cover. The charnockite contains abundant quartz and alkali feldspar. The orthopyroxene is an inverted pigeonite, occasionally extremely Fe-rich (En_{18}). The accessory minerals are apatite, zircon and rarely sphene and allanite. The petrological data (DEMAÏFFE, 1977b) indicate that this material might correspond—at least qualitatively—with the late stage residual liquid of the anorthosite differentiation process.

The contact of the Hidra body with the granulite facies gneisses is outlined by a fine-grained (300–500 μm) rock of jotunitic character (jotunite = hypersthene monzodiorite). The transition from leuconorite to jotunite is very progressive. The proportion of cumulate plagioclase decreases while the amount of mesostasis increases towards the border. The jotunite locally contains plagioclase phenocrysts (up to 2 cm), slightly zoned and showing the bluish cast typical of anorthositic plagioclase; their mean An content is 45%. On the basis of field relations and petrological data, the fine-grained border jotunite may be interpreted as a magmatic liquid intimately associated with the plagioclase cumulates. Most likely, it is equivalent with the chilled margin of shallower intrusions.

It follows from the composition of the major minerals (An-content of the plagioclase and En-content of the orthopyroxene) that the anorthosite crystallized first, followed

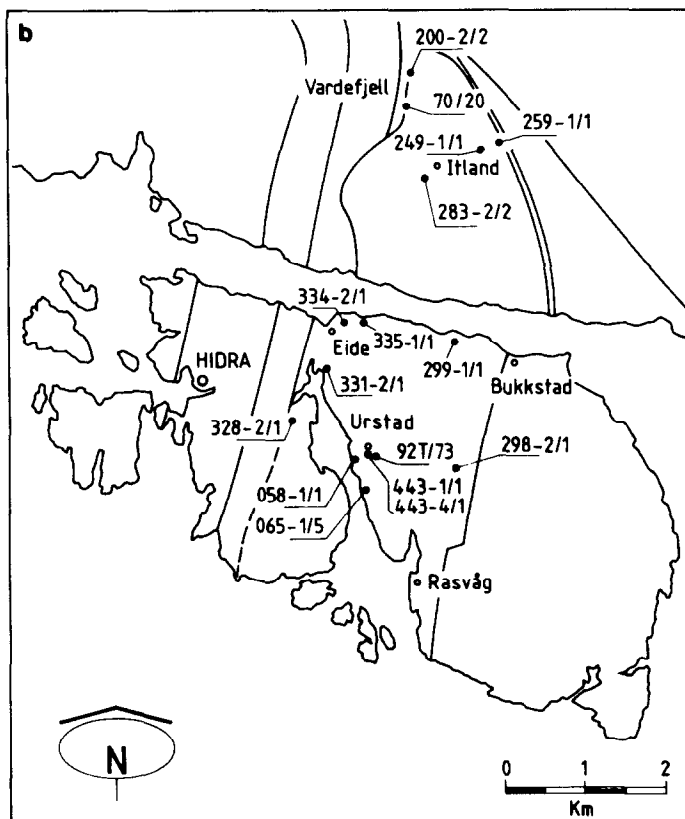


Fig. 1b. Sample locations; see Table 1 for sample type.

by the leuconorite (Fig. 3). However, the proportions of the various rock types are difficult to assess with good precision, as the Hidra body lacks a stratiform structure. From the outcrop ratios, deduced from a detailed geological map, the proportion of anorthosite has been tentatively estimated at 35%; the remaining being leuconorite and charnockite. It is very difficult to estimate the proportion of charnockitic material from field data alone; it is definitely greater than 10% and probably less than 25%.

The average mineralogy of the cumulate phases in the leuconorite can be derived from the actual mineralogical composition, as there is no layering due to crystal sorting. Moreover, there is no petrographical evidence for the presence of a trapped liquid in the cumulate leuconorites. The anorthosites, on the contrary, are characterized by an orthocumulate texture, so that the actual mineralogical composition of the anorthosites is not the same as the original cumulate mineralogy. The latter has been estimated from the modal or the normative composition by subtracting the late stage minerals quartz, K-feldspar and biotite, which crystallized from the intercumulus liquid. The adopted average mineralogy is 82% plag + 10% opx + 7% Fe-Ti oxides + 1% apatite for anorthosites, and 52% plag + 24% opx + 8% cpx + 15% Fe-Ti oxides + 1% apatite for leuconorites. It needs to be emphasized that these figures are averages, and that there are considerable sample-to-sample variations in the modal composition of the cumulate rocks.

ANALYTICAL METHODS

Mass spectrometry

The isotopic composition of Sr separated on ion exchange column has been measured by thermoionisation on single rhenium filaments with a TH5 VARIAN MAT

mass spectrometer from the 'Centre Belge de Géochronologie'. Values are normalized to a $^{86}\text{Sr}/^{88}\text{Sr}$ ratio of 0.1194. Ten determinations of the Eimer and Amend Sr standard yield an average value of $^{87}\text{Sr}/^{86}\text{Sr} = 0.70807 \pm 7$ (1σ); the NBS 987 Sr standard gives as a mean $^{87}\text{Sr}/^{86}\text{Sr} = 0.71015 \pm 4$ (1σ) for 7 measurements. Rb and Sr were determined by isotope dilution in all the samples analyzed for the isotopic composition of Sr (with the exception of the charnockites).

Instrumental neutron activation analysis

The samples (*ca.* 1 g) were irradiated for *ca.* 7 hr at a thermal neutron flux of *ca.* $2.10^{12} \text{ n} \cdot \text{cm}^{-2} \cdot \text{s}^{-1}$ in the Thetis reactor of the Institute of Nuclear Sciences, Gent University. The induced gamma-ray activities were measured with large volume coaxial Ge(Li) detectors and a planar 0.4 cm³ extra high-resolution low Energy Ge(Li) Detector (LEPD) (HERTOGEN and GJIBELS, 1971). In some samples dysprosium was determined via 2.35 hr ^{165}Dy after a 10 min irradiation. To ensure reproducible irradiation and counting geometry, the samples were prepared as pellets; spectrographically pure graphite and, in later stages of the work, a dry hydrocarbon wax powder was used as a binder. USGS AGV-1 reference rock or secondary in-house reference rocks were used as standards.

Other methods

Samples J70/20 and JP70/20 have been analyzed for trace elements by I. Roelands (Liège University) via radiochemical and epithermal neutron activation analysis during a stay at Oslo University. The results have been published in DUCHESNE *et al.* (1974) and are included in Tables 1-3 for easy reference.

The major element composition of all samples except PY 328-2/1 has been determined by C. Chaval (Brussels University) by wet chemical methods. X-Ray fluorescence (M.

Delvigne and F. Durez, Museum of Central Africa, Tervuren, Belgium) was used for the major element analysis of PY 328-2/1 and for the determination of the Rb and Sr contents of the charnockites and the samples for which no Sr isotopic data are listed in Table 2.

SAMPLES AND DATA

The major element composition of the whole rocks analyzed are listed in Table 1, and the trace element and isotopic data in Tables 2 and 3. The chondrite-normalized REE patterns are shown in Figs 4 and 5. In addition to whole rocks, Tables 2 and 3 also include results for separated plagioclase crystals and an orthopyroxene megacryst. Sample locations are shown in Fig. 1b.

Samples APO65-1/5 and AP443-1/1 are the unzoned central parts of two large plagioclase crystals from ortho-cumulate anorthosites. JP70/20 and JP200-2/2 are composite samples of several plagioclase phenocrysts separated

from jotunites J70/20 and J200-2/2. Sample L92T/73 is a leucotroctolite; it has ca. 20% modal olivine and low modal orthopyroxene. Leucotroctolites are rarely observed in the Hydra massif. PY328-2/1 is a pyroxenitic enclave found in leuconorite. The orthopyroxene megacryst OP404-4/1 (En₆₈) comes from the Garsaknatt Massif, another sub-unit of the Rogaland Complex. The Garsaknatt Massif is very similar to the Hydra body in many respects: structure, petrology, REE geochemistry and Sr isotopic composition (DEMAÏFFE, 1977a). This sample was included to estimate orthopyroxene/liquid partition coefficients.

The heterogeneous and very coarse-grained granitic pegmatites have not been analyzed for trace elements, because it is exceedingly difficult to prepare a representative sample. However, ADAMSON (1942) showed that these pegmatites contain numerous REE bearing minerals, especially those enriched in heavy REE (xenotime, euxenite, gadolinite, etc.).

Table 1. Major element composition of rocks from the Hydra Massif[†]

	335-1/1 A	058-1/1 A	299-1/1 A	92T/73 L	334-1/1 L	331-2/1 L	249-1/1 L
SiO ₂	52.6	57.6	59.8	48.0	46.2	48.3	49.5
TiO ₂	1.15	0.58	0.45	1.35	5.20	5.60	2.60
Al ₂ O ₃	25.0	23.6	20.9	22.7	15.9	14.7	13.8
Fe ₂ O ₃	1.36	1.50	0.68	2.3	5.75	2.67	3.24
FeO	2.91	1.45	2.78	5.6	10.72	11.83	10.6
MgO	2.40	1.12	1.36	5.0	5.68	7.04	9.68
MnO	-	-	-	0.12	-	-	-
CaO	9.32	8.40	5.96	9.12	7.64	7.00	6.88
Na ₂ O	4.42	4.32	4.30	3.84	3.06	2.64	2.55
K ₂ O	0.66	1.75	2.34	0.56	0.64	0.44	0.50
H ₂ O	0.49	0.64	0.80	0.50	0.05	0.50	0.53
P ₂ O ₅	0.11	0.14	0.20	-	0.19	0.05	0.10
Total	100.40	101.10	99.60	99.10	101.00	100.80	100.00
	328-2/1 PY	200-2/2 J	70/20 J	259-1/1 J	443-4/1 C	283-2/2 C	298-2/1 C
SiO ₂	37.4	48.7	48.0	49.80	55.2	65.5	67.2
TiO ₂	9.7	4.12	4.61	4.28	2.12	0.70	0.75
Al ₂ O ₃	2.60	12.4	14.2	14.10	17.4	14.65	14.4
Fe ₂ O ₃	11.10	4.70	5.0	2.20	3.63	3.46	3.64
FeO	20.62	12.39	10.40	11.70	5.26	2.65	1.21
MgO	13.65	6.00	4.60	4.90	2.12	0.86	0.40
MnO	0.32	-	0.18	0.17	-	-	-
CaO	1.91	6.04	6.41	6.00	5.60	3.44	2.80
Na ₂ O	0.40	3.24	3.65	3.50	4.50	3.60	2.96
K ₂ O	0.15	1.32	1.08	1.95	3.06	4.80	5.18
H ₂ O	-	0.70	0.95	0.32	0.31	0.90	0.56
P ₂ O ₅	0.11	0.40	0.80	0.91	0.19	-	0.12
Total	98.00	100.00	99.90	99.80	99.40	100.60	99.20

[†] A=anorthosite; L=leuconorite; PY=pyroxenite; J=jotunite; C=charnockite

Table 2. Trace element and Sr-isotopic composition of rocks from the Hydra Massif

	Sc	Cr	Co	Rb	Sr	Hf	Ta	Th	U	K/Rb	Rb/Sr	(87/86) _c
A 335-1/1	5.3	10	20.3	6	807	0.62	0.18	0.36	-	913	0.0074	-
A 058-1/1	4.4	-	6.4	34	722	4.3	-	1.3	0.58	440	0.047	0.7057
A 299-1/1	5.7	-	17.8	66	572	9.7	-	1.9	0.56	305	0.115	-
AP 065-1/5	0.31	<5	1.8	4.4	915	0.15	0.02	0.18	<0.1	943	0.0048	0.7053
AP 443-1/1	0.38	<5	2.6	7.6	908	0.20	0.02	0.12	<0.1	700	0.0084	0.7053
L 92T/73	3.7	380	50.	7.3	1206	0.68	0.16	0.26	-	636	0.0061	-
L 334-1/1	17.9	10	68.	2	475	2.3	0.63	0.82	-	2655	0.0042	0.7058
L 331-2/1	21.1	-	78.	3.8	425	1.3	-	<0.1	<0.2	912	0.0088	-
L 249-1/1	18.8	-	70.	7.7	438	1.5	-	0.44	<0.2	539	0.018	0.7055
PY 328-2/1	34.5	42	79.	5.6	48	2.0	0.83	0.29	0.16	222	0.116	-
OP 404-4/1	33.8	-	105.	-	-	0.39	-	0.05	<0.1	-	-	-
J 70/20	-	-	-	19.	453	-	-	2.0	0.85	462	0.043	0.7061
J 200-2/2	25.9	-	47.	23.	372	4.5	-	1.2	0.21	487	0.061	-
J 259-1/1	19.7	-	47.	44.	381	8.2	-	3.8	1.3	368	0.115	0.7052
JP 70/20	1.69	-	7.3	3.6	784	0.6	-	0.35	0.10	1450	0.0046	0.7053
JP 200-2/2	1.57	-	12.2	7.4	684	0.66	-	0.17	-	450	0.011	0.7055
C 443-4/1	21.1	25	16.0	85.	420	34.	1.6	9.8	3.0	300	0.212	0.7086 [†]
C 283-2/2	14.2	14	8.4	148.	299	18.	0.53	2.2	0.63	269	0.495	0.7086 [†]
C 298-2/1	8.3	8	6.4	282.	238	21.	0.72	21.	0.90	152	1.18	0.7086 [†]

[†] Initial ratios derived from a whole rock isochron (see text for discussion).

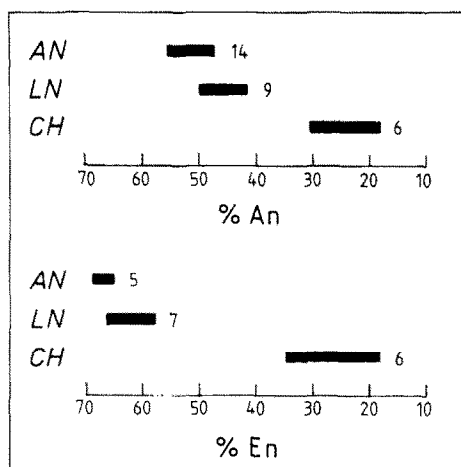


Fig. 3. Compositional ranges of plagioclase and orthopyroxene in anorthositic orthocumulates (AN), leuconoritic adcumulates (LN) and charnockites (CH). The data show that the anorthosites crystallized before the leuconorites. Figures are the number of samples studied.

STRONTIUM ISOTOPIC COMPOSITION

The comagmatic character of the main rock types of the Hidra body has been checked by measuring the Sr-isotopic composition (Table 2). The initial isotopic ratios are low in the intrusive anorthositic-noritic rocks (0.7035–0.7065; DEMAIFFE *et al.*, 1974; DEMAIFFE, 1977a), but much higher in the surrounding gneissic rocks (0.715–0.720; VERSTEEVE, 1975). The initial ratios of the jotunitites, anorthosites, leuconorites and plagioclase crystals have been calculated from the measured ratio, after correction for *in situ* decay of ^{87}Rb during 909 Ma, the age of the massif. For most samples, the Rb/Sr ratio is so low that this correction is not very important. The Hidra jotunitites and plagioclase cumulates have the same initial ratio: 0.7055 ± 0.0004 (mean of 9 values), implying that they really belong to the same magmatic unit. Field relations led to the same conclusion.

The initial Sr-isotopic ratio of the charnockites and pegmatites has been derived from a 6 points (4 char-

nockites and 2 pegmatites) Rb–Sr whole rock isochron, which yields an age of 909 ± 25 Ma and $(^{87}\text{Sr}/^{86}\text{Sr})_0 = 0.7086 \pm 0.0006$ (2σ) (see Fig. 6 in DEMAIFFE *et al.*, 1979). The initial ratios are higher than in the jotunitites and the anorthosites, but are much lower than in the surrounding gneisses 909 Ma years ago ($^{87}\text{Sr}/^{86}\text{Sr} = 0.720$ – 0.725 ; VERSTEEVE, 1975). Most probably, the charnockites have been contaminated by supracrustal material, as is also evident from the K/Rb evolution (DEMAIFFE *et al.*, 1979) and oxygen isotopic composition (DEMAIFFE and JAVOY, 1980).

TRACE ELEMENTS

Rare earth elements (REE), Hf, Ta, Th and U

The REE data are shown in Figs 4 and 5. The plagioclase crystals separated from anorthosites have low REE abundances, a pronounced positive Eu-anomaly ($\text{Eu}/\text{Eu}^* = 7.8$), and a highly fractionated REE pattern ($\text{La}/\text{Yb}_N = 18.5$). They lie within the range of plagioclase from massif anorthosites (GRIFIN *et al.*, 1974). The steep REE pattern reflects the preferential uptake of the light REE in plagioclase (e.g. SCHNETZLER and PHILPOTTS, 1970; IRVING, 1978) and the crystallization from a LREE enriched liquid.

The plagioclase phenocrysts separated from jotunitites have markedly higher REE contents than anorthositic plagioclase of nearly equal An-content; but the two types of plagioclases have virtually the same relative pattern. The very high La concentrations of the phenocrysts (Table 3; Fig. 5) are a particularly puzzling feature. Since samples JP70/20 and JP200-2/2 have been analyzed in two different laboratories, using different standards, standardization errors can be ruled out. Contamination with La during sample preparation also appears an implausible cause (e.g. the La/Ce ratios are the same in the two samples). Plagioclase phenocrysts from the jotunitites were slightly zoned and not completely free from REE rich matrix material. However, it is unlikely that the overall higher REE abundances are simply due to contamination with jotunitic matrix, since this would

Table 3. Rare Earth Element content of rocks from the Hidra Massif

	La	Ce	Nd	Sm	Eu	Gd	Tb	Yb	Lu	(La/Yb) §	Eu/Eu †
A 335-1/1	4.5	9.0	4.9	0.92	1.27	-	0.13	0.32	0.054	8.23	4.4
A 058-1/1	14.5	35.	20.	3.7	1.88	3.3	0.56	1.59	0.24	5.39	1.70
A 299-1/1	27.7	62.	37.	7.2	2.87	5.8	1.11	3.1	0.49	5.31	1.34
AP 065-1/5	4.0	8.0	3.9	0.63	1.40	-	0.071	0.128	-	18.3	7.8
AP 443-1/1	4.7	8.7	4.7	0.73	1.64	-	0.094	0.148	-	18.7	7.7
L 92T/73	5.1	10.5	6.7	1.26	1.07	-	0.18	0.30	0.06	9.97	2.6
L 334-1/1	7.4	18.1	10.9	2.36	1.26	-	0.39	1.05	0.14	4.16	1.6
L 331-2/1	1.6	4.3	2.4	0.61	0.67	0.83	0.14	0.53	0.085	1.73	2.89
L 249-1/1	5.4	12.1	6.9	1.54	0.86	1.3	0.29	0.80	0.13	3.95	1.78
PY 328-2/1	1.35	3.8	2.9	0.69	0.25	-	0.18	0.93	0.17	0.86	1.0
OP 404-4/1	0.36	-	-	0.30	0.10	-	0.10	0.70	0.17	0.30	0.80
J 70/20	30.3	75.	47.	11.7	3.35	-	1.58	3.2	0.54	5.58	0.92
J 200-2/2	21.3	49.	29.	6.6	2.27	6.6	1.04	3.6	0.63	3.54	1.0
J 259-1/1	33.9	82.	52.	11.3	3.31	11.1	1.69	3.5	0.52	5.71	0.92
JP 70/20	37.2	18.	7.1	1.49	2.86	-	0.16	0.31	0.047	17 †	7.1
JP 200-2/2	50.3	26.	9.4	1.27	3.10	0.91	0.127	0.26	0.036	34 †	9.0
C 443-4/1	71.6	166.	108.	21.9	3.82	-	3.6	10.3	1.64	4.11	0.55
C 283-2/2	72.6	169.	107.	20.3	2.94	-	2.9	6.3	0.92	6.83	0.47
C 298-2/1	108.	266.	98.	14.7	1.96	-	1.62	4.3	0.67	15.0	0.50

(La/Yb) § : chondrite-normalized ratio; † : extrapolated from Ce/Yb ratio.

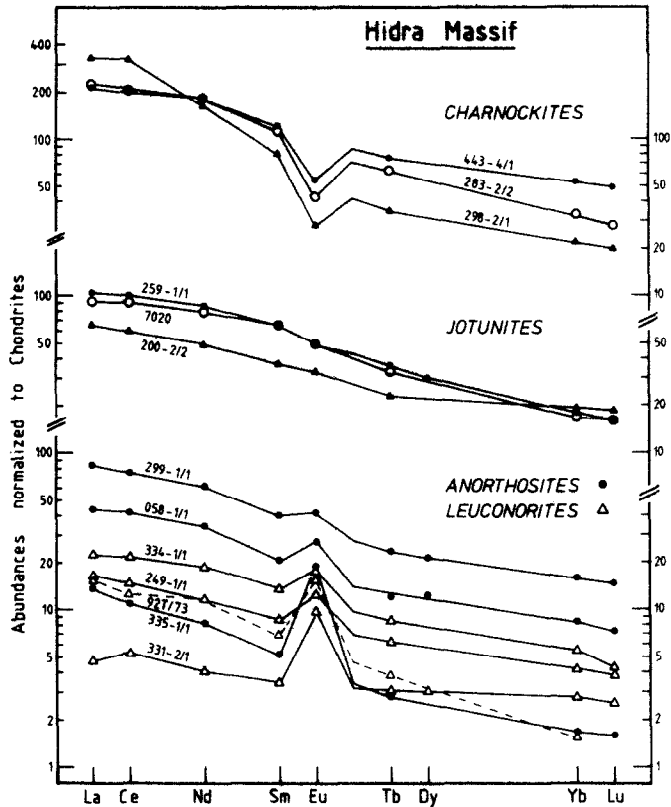


Fig. 4. Chondrite-normalized REE patterns of the whole rock samples.

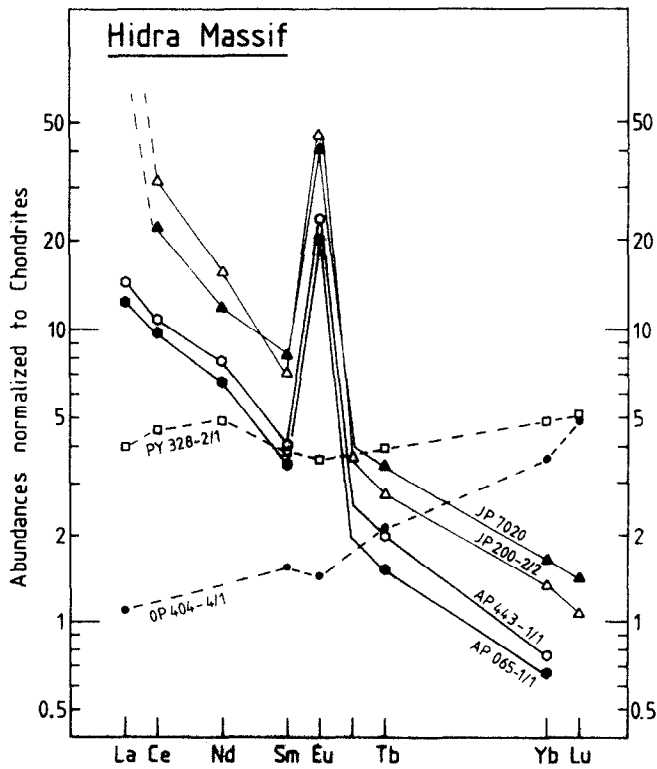


Fig. 5. Chondrite-normalized REE patterns of the unzoned cores of two large plagioclase crystals from anorthositic orthocumulates (AP) and or two composite plagioclase phenocryst samples from the border jotunites (JP). See text for discussion of the high La contents of the plagioclase phenocrysts. Also plotted are the data for a pyroxenite (PY) and an orthopyroxene (OP) megacryst.

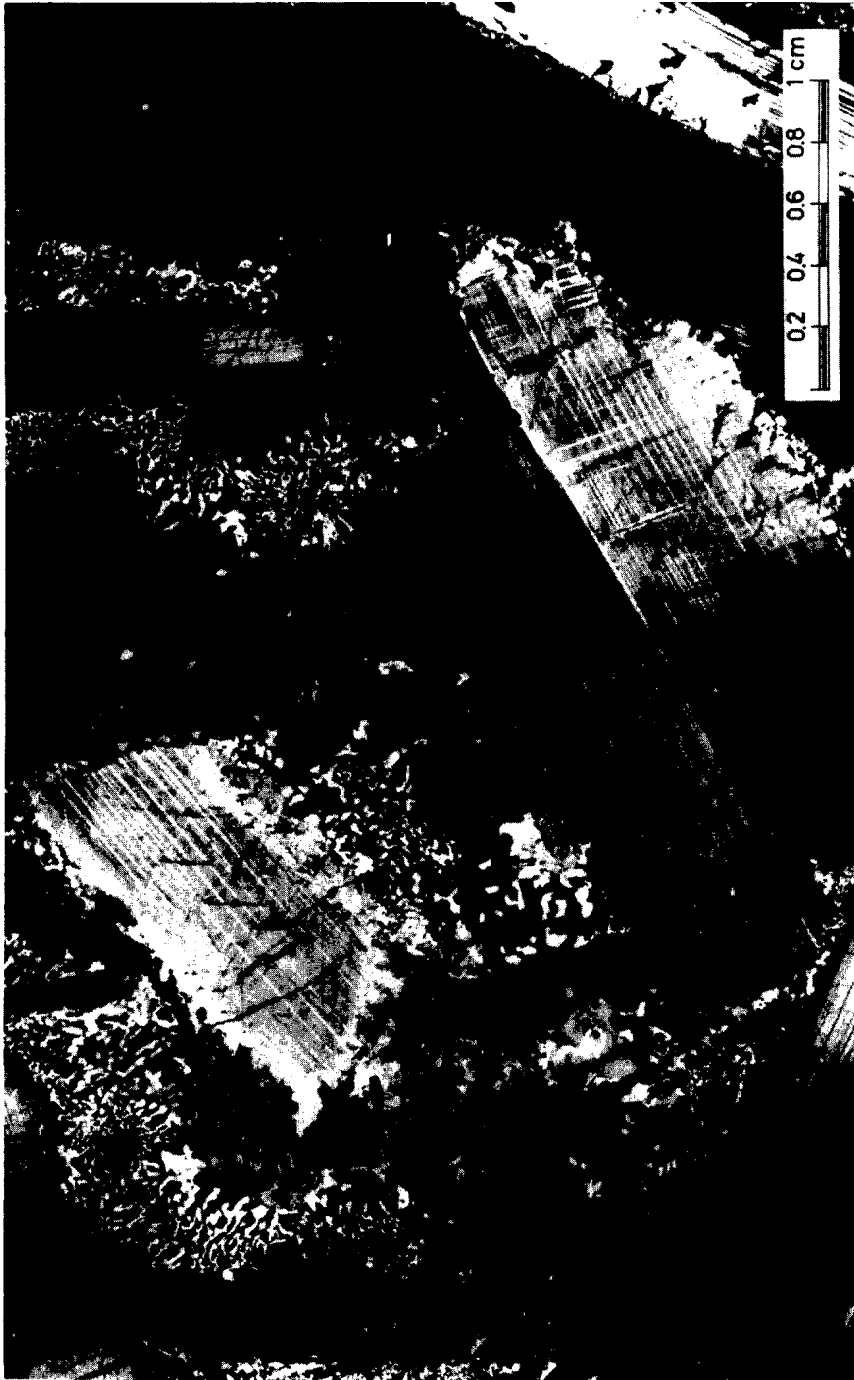


Fig. 2. Photomicrograph of a typical orthocumulate anorthosite. The trapped intercumulus liquid crystallized as a thin zoned border on the cumulus plagioclases and as a finer grained mesostasis consisting of quartz and K-feldspar micrographic intergrowths.

tend to lower the Eu/Eu^* and La/Yb_N ratios relative to pure plagioclase, contrary to observation.

Plagioclase minerals ($\text{An} < 60$) from massif type anorthosites have 5 to 10 times higher REE abundances than plagioclase minerals from Archean calcic anorthosites ($\text{An} 65\text{--}95$), such as the Fiskenaesset (HENDERSON *et al.*, 1976) and Shawmere (SIMMONS *et al.*, 1980) Complexes. The REE data highlight the profound geochemical and petrogenetic differences between these two types of anorthosites.

The LREE depleted orthopyroxene (OP 404-4/1) pattern is in keeping with available partition coefficient data (IRVING, 1978). The pyroxenite (PY 328)2/1 has higher LREE contents, presumably due to the small amounts of plagioclase, oxides and apatite present in the sample.

The positive Eu-anomalies of the anorthosites and leuconorites are typical of rocks formed by accumulation of plagioclase crystals. The REE patterns are very similar to those reported by PHILPOTTS *et al.* (1966), GREEN *et al.* (1972), SIMMONS and HANSON (1978) and ASHWAL and SEIFERT (1980) for other anorthositic massifs.

As stated earlier, the mineralogical data (Fig. 3) show that anorthosites crystallized before the leuconorites. As the first rocks formed, the anorthosites are then expected to have the lowest REE abundances and the largest positive Eu-anomalies. Two out of the three anorthosites analyzed actually have higher REE (and other incompatible element) concentrations than the leuconorites. This aspect sets the Hidra anorthosites apart from the Nain-Adirondacks and Lofoten-Vesteraalen anorthosites (SIMMONS and HANSON, 1978; GREEN *et al.*, 1972). The trace element patterns of many Hidra anorthosites are largely determined by the trapped intercumulus liquid, which gave rise to the orthocumulate textures. The REE patterns then depend on the proportion and on the degree of fractionation of the intercumulus liquid at the very moment of solidification.

The main geochemical features of the jotunites are a smooth REE pattern without Eu-anomaly (J200-2/2), or only a very small one (J70/20 and J259-1/1). The jotunites thus neither gained nor lost appreciable amount of plagioclase, and appear therefore the least fractionated components of the Hidra Massif.

The charnockitic dykes are strongly enriched in REE and have a pronounced negative Eu-anomaly. Their trend is complementary to that of the plagioclase cumulates. On the basis of major and trace elements, the three charnockites appear to be samples of a charnockitic fractional crystallization sequence. Most likely, the decrease of the heavy REE with increasing differentiation has to be attributed to crystallization of zircon, as it is the only ubiquitous mineral in which the HREE are strongly enriched (NAGASAWA, 1970; WATSON, 1980).

As incompatible lithophile elements, Hf, Ta, Th and U generally follow the light REE (Tables 2 and 3).

However, the distribution pattern of the charnockites is complex. The most differentiated samples C283-2/2 and C298-2/1 have lower Hf, Ta and U contents than sample C443-4/1. It is quite conceivable that the behaviour of these trace elements in the charnockites has been largely controlled by the accessory minerals. The charnockites also have markedly higher Hf/Ta ratios (20–35) than the other samples for which Ta data are available (2.5–10). Th/U ratios are within the common range (2–6) for all samples, except for charnockite C298-2/1 ($\text{Th}/\text{U} = 23$).

Rubidium, strontium and potassium. Plagioclase readily accommodates Sr and excludes Rb. These two elements are therefore strongly fractionated in our suite of samples, which encompasses plagioclase crystals, plagioclase-rich cumulates and liquids that crystallized appreciable amounts of plagioclase. With the exception of pyroxenite PY328-2/1, the Sr contents do not vary by more than a factor of three; the Rb concentrations, on the other hand, cover almost two orders of magnitude. The variation of the Rb abundances is therefore the main cause of the large spread of the Rb/Sr ratios, as shown in Fig. 6. It is worthwhile to note that the plagioclase phenocrysts from the jotunites are not richer in Rb than the plagioclase crystals from anorthosites. It is another indication that the higher REE contents of the jotunite phenocrysts (Fig. 5) are not due to matrix contamination.

The K/Rb ratios are inversely proportional to Rb content (Table 2). K/Rb ratios are high in the leuconoritic cumulates due to the high modal abundances

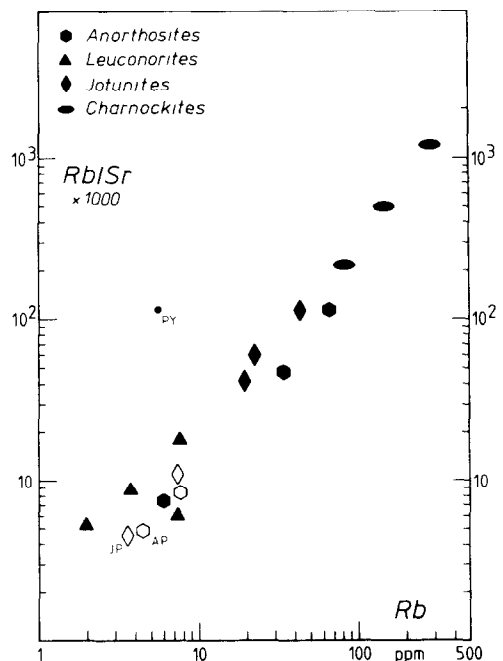


Fig. 6. The variation of the Rb/Sr ratios is largely determined by the highly variable Rb contents. AP = plagioclase crystals from anorthositic orthocumulates; JP = plagioclase phenocrysts from jotunites; PY = pyroxenite 328-2/1.

of plagioclase with characteristically high K/Rb ratios (MURTHY and GRIFFIN, 1970). The K and Rb contents and the K/Rb ratios of the anorthosites depend upon the amount of trapped liquid. The charnockites are much more enriched in Rb and K, hence the low K/Rb ratios.

Scandium and cobalt. In the cumulate rocks, the concentration of these two compatible elements depends upon the modal abundance of pyroxene. The low Sc content of leucotroctolite L92T/73 reflects the presence of olivine instead of orthopyroxene as the main ferromagnesian mineral. The decline of the Sc and Co contents with increasing degree of differentiation of the charnockites can be ascribed to protracted crystallization of pyroxene and/or opaque minerals.

A JOTUNITIC PARENTAL MAGMA OF THE HIDRA MASSIF

Field observations, petrographical data and the geochemical characteristics of the different rock types suggest that the jotunitites are the most likely parental magma of the Hidra body. Firstly, there is the occurrence as a fine-grained border facies, and the progressive transition to leuconorites. Secondly, the absence of an Eu-anomaly precludes that the jotunitites are a residual magma formed after crystallization of substantial amounts of plagioclase. Thirdly, the complementary REE patterns of the anorthositic cumulates and the strongly differentiated charnockites are most readily explained by fractional crystallization of an intermediate, jotunitic magma. All these characteristics are the earmarks of a chilled parental magma margin.

Parental magmas of andesine-type massif anorthosites have never been unequivocally recognized as such in the field. It is thus not surprising that there is little agreement on the nature and origin of the parental magmas. Jotunitic (or monzodioritic) magmas are not generally accepted as parental magmas of massif type anorthosites, and the comagmatic character of anorthositic rocks and associated charnockites is often disputed (e.g. BUDDINGTON, 1969; EMSLIE, 1978). For example, in their recent geochemical studies of the Adirondacks anorthosites SIMMONS and HANSON (1978) and WIEBE (1980) proposed gabbroic anorthositic parental magmas, while ASHWAL and SEIFERT (1980) argued that the residual liquid of the anorthositic differentiation is represented by mafic olivine-bearing dykes, rich in Fe, Ti-oxides and REE, and not by silicic charnockites.

Many authors favor Al-rich ($Al_2O_3 \geq 20\%$) parental magmas, because they can produce abundant anorthosite-rich cumulates without a large complementary ferromagnesian fraction. Indeed, available gravity data suggest that most anorthositic plutons do not have large volumes of mafic cumulate layers at their roots. Nevertheless, a model based on the assumption that the parental magma of the Hidra Massif was a gabbroic anorthosite will meet serious

difficulties, because it offers no straight-forward explanation for the occurrence and geochemical characteristics of the jotunitic border facies. A gabbroic anorthositic magma can only give rise to monzodioritic residual liquids through protracted crystallization of plagioclase. The Hidra jotunitites lack the negative Eu-anomalies which would result from such a fractionation process. ASHWAL and SEIFERT (1980) questioned the significance of the lack of an Eu-anomaly in the Hidra jotunitites. They claimed that this could be the fortuitous result of mixing liquids having negative anomalies with cumulates having positive anomalies. However, we find it highly improbable that the occurrence of the jotunitites at the border of the Hidra Massif and the progressive transition to leuconorites are the fortuitous result of an accidental mixing process too.

EMSLIE (1978) discussed the origin of the jotunitites in some detail. He interpreted the jotunitites as residual magmas remaining after high-pressure olivine plus orthopyroxene fractionation of a basic magma. As similar basic magmas are considered as the starting material of the Al-rich parental magmas of anorthosites, the jotunitites are related to but not strictly comagmatic with the anorthosites. This model might be a viable one for those jotunitites that appear as small dykes and intrusions in several anorthosites, but it fails to account for the progressive transition of the Hidra border jotunitites to leuconorites.

On the basis of field observations and experimental data, PHILPOTTS (1978) and WIEBE (1979) recently proposed that the late stage residual liquid of the anorthosite fractionation could split into immiscible iron-rich and silica-rich fractions. Applied to the Hidra Massif, the 'ferrodioritic' iron-rich liquid would be the equivalent of the jotunitites, the silica-rich liquid the equivalent of the charnockites. Again, this model cannot be reconciled with our field observations and geochemical data. The immiscibility hypothesis can hardly explain the occurrence of jotunitites as a border facies, and the smooth transition to leuconorite. Immiscibility textures, such as ocellae of one rock type into the other, have never been observed in the jotunitites and charnockites. These rocks never occur in close proximity in the field. Moreover, available experimental data show that the REE are enriched in the basic melt relative to the coexisting immiscible silicic melt (WATSON, 1976; RYERSON and HESS, 1978); the Hidra jotunitites and charnockites show exactly the opposite distribution. Finally, the distinctly different strontium initial isotopic ratios (Table 2) seem to rule out that the Hidra jotunitites and charnockites are conjugate immiscible liquids.

MODELLING OF REE FRACTIONATION DURING CRYSTALLIZATION OF THE HIDRA MASSIF

Our hypothesis that the Hidra anorthosite-charnockite suite resulted from fractional crystallization of

a jotunitic parental magma can be semi-quantitatively evaluated using trace element and major element constraints. We will first show that the model reproduces the REE patterns of the cumulate rocks and residual charnockites. Jotunitic 200-2/2 has been chosen as representative for the parental magma, as it appeared to be the least fractionated of the three jotunitic analyzed (e.g. lower LREE, higher MgO and Mg/Mg + Fe²⁺ ratios; Tables 1-3).

Crystallization stages

The fractional crystallization process has been formally divided in two main stages, based on field relationships and petrographical data (Fig. 3): an 'anorthositic' stage from 0 to 35% crystallization, followed by a 'leuconoritic' stage. The proportions of the precipitating minerals (Table 4) have been derived from the *average* cumulate mineralogy, as discussed earlier (Geology and petrography...). These proportions were kept constant in each crystallization stage. This is obviously an oversimplification, especially for high degrees of solidification when the proportions of accessory minerals are expected to increase.

Partition coefficients

The solid/liquid partition coefficients adopted in this study are summarized in Table 5. Since plagioclase is the major mineral in both the anorthositic and the leuconoritic stages, the model calculations will critically depend on the choice of appropriate plagioclase partition coefficients. The values used here were obtained by dividing the measured concentrations in the unzoned cores of the large plagioclase crystals AP065-1/1 and AP443-1/1 by the concentrations in jotunitic 200-2/2, the proposed parental magma. These partition coefficients are remarkably similar to the experimentally determined values of DRAKE and WEILL (1975) at 1150 C. This temperature appears also the most appropriate one, because it is close to the estimated 1100 C (DEMAIFFE, 1977a) of plagioclase crystallization in the porphyritic jotunitic, judging from the KUDO-WEILL (1970) geothermometer.

One could argue that partition coefficients calculated from the plagioclase phenocryst-jotunitic pairs are more relevant to the problem at hand. Disregarding for a moment the anomalously high La contents of the phenocryst samples, partition coefficients derived in this way are about two times higher than those listed in Table 5 (see also Table 3 and Fig. 5). Such high values are outside the range of experimentally determined coefficients (DRAKE and WEILL, 1975; WEILL and MCKAY, 1975), and have only rarely been observed for phenocryst-matrix pairs (e.g. SCHNITZLER and PHILPOTTS, 1970). It is tempting to ascribe the higher REE concentrations in the jotunitic phenocrysts to contamination with REE-rich matrix material. However, the virtually identical Ce/Yb ratios and Eu-anomalies (Fig. 5) and the lack of a Rb enrichment (Fig. 6) in the jotunitic phenocrysts, as compared to plagioclase mega-

Table 5.
Solid/liquid REE partition coefficients
adopted in the model calculations

	Plag	Opx	Cpx	Ilm	Mag	Ap
La	0.203	0.017	0.06	0.015	0.006	4.3
Ce	0.172	0.022	0.11	0.016	0.006	5.5
Nd	0.148	0.029	0.21	0.017	0.006	6.9
Sm	0.103	0.045	0.34	0.018	0.006	7.3
Eu	+	0.045	0.34	0.018	0.006	6.0
Tb	0.080	0.096	0.44	0.019	0.006	7.7
Yb	0.040	0.200	0.40	0.034	0.008	4.1

+ K = 0.5 + 0.5xP (see text for discussion)

crysts, are not consistent with simple matrix contamination. More likely, the high REE contents—especially the anomalously high La abundances—of the jotunitic phenocrysts reflect departure from equilibrium in the rapidly crystallized fine-grained jotunitic border facies (ALBAREDE and BOTTINGA, 1972; HENDERSON and WILLIAMS, 1979).

The orthopyroxene REE partition coefficients are the concentrations in the orthopyroxene megacrysts 404-4:1, normalized to jotunitic 200-2/2. Admittedly, this approach is not entirely accurate, as the exact relationships between the jotunitic magma and the orthopyroxenite are not known. The partition coefficients for the light REE are about two times higher than the experimentally determined values of WEILL and MCKAY (1975) at 1200 C, but are within the range of published values.

For the less abundant minerals (clinopyroxene, oxides, apatite) we have adopted the values deduced by J. C. DUCHESNE (personal communication) from the measured REE concentration in minerals of a cumulate norite from the Bjerkrem Sogndal layered lopolith (DUCHESNE, 1978). The ilmenite and clinopyroxene mineral/liquid partition coefficients are comparable to the experimental data of MCKAY and WEILL (1976) and GRUTZECK *et al.* (1974), respectively. The magnetite partition coefficients are as yet ill-defined. The values listed in Table 5 could admittedly be lower limits, because the magnetite formed from a liquid depleted in REE as a result of apatite crystallization. However, it is doubtful whether the fairly high (>1) magnetite REE partition coefficients inferred by SCHOCK (1979) are applicable to the Hidra rocks. For example, it would be rather difficult to explain the relatively low light REE abundances of pyroxenite 328-2:1, which contains *ca.* 16% modal magnetite. In spite of its low modal abundance, apatite contributes significantly to the overall solid/liquid REE distribution coefficients. Fortunately, even changes by a factor of two in the partition coefficients or modal abundance of apatite do not basically affect the final outcome of the model calculations.

Though there is now ample experimental evidence that partition coefficients are temperature and composition dependent (IRVING, 1978; and references cited herein), the crystallization history of the Hidra body is not well enough constrained to accommodate available partition coefficient-temperature-composition relationships in the calculations. We therefore assumed that the partition coefficients remained constant. An exception was made for the Eu plagioclase/liquid partition coefficient. Indeed, the compositional variations of the oxide minerals in the Hidra body is very similar to the variations in the Bjerkrem-Sogndal lopolith, and appear to reflect a decreasing oxygen fugacity with increasing solidification (DUCHESNE, 1972). Consequently, the Eu²⁺/Eu³⁺ ratio and K_{Eu}^{pl,ox} increased systematically. Moreover, the Eu²⁺ plagioclase partition coefficient (as inferred from its analogue Sr²⁺) appears to increase more rapidly than K_{Sm}^{pl,ox} and K_{Gd}^{pl,ox} with falling temperature (DRAKE and WEILL, 1975). As a first order approximation we assumed that the Eu plagioclase partition coefficient varied as K_{Eu}^{pl,ox} = 0.5 + 0.5 × F.

Table 4
Proportions (%) of
crystallizing minerals

	A	B
	F < 35 %	F > 35 %
plagioclase	82	52
orthopyroxene	10	24
clinopyroxene	-	8
Fe, Ti-oxides	7	15
apatite	1	1

A = anorthositic stage;

B = leuconoritic stage;

F = degree of solidification.

Fractionation equations

The trace element variation trends in the residual liquid which fractionates according to a Rayleigh model, is calculated from:

$$C^L(F) = C(0)(1 - F)^{D-1} \quad (1)$$

wherein: $C(0)$ = concentration in the parental magma; $C^L(F)$ = concentration in the residual liquid; F = degree of solidification ($0 \leq F \leq 1$); $D = \sum p_i K_i$ = bulk distribution coefficient; K_i = solid/liquid partition coefficient of precipitating mineral i ; p_i = proportion of mineral i in the precipitating assemblage. Equation (1) is valid for $D = \text{constant}$, i.e. for constant p_i 's and K_i 's. Results for several crystallization stages, having different but constant D 's, can be readily obtained by considering the liquid at the end of stage i as the parental liquid for stage $i + 1$, and so on, and using appropriate values for F .

To calculate the fractionation of Eu in the present case, eqn (1) has to be modified to account for the variable plagioclase partition coefficient. When the partition coefficient of one or more minerals linearly varies with F , the bulk distribution coefficient takes the form $D(F) = D_0 + aF$. Solution of the generalized differential equation for Rayleigh fractionation gives:

$$C^L(F) = C(0)(1 - F)^{(D_0 + a-1)} e^{aF} \quad (2)$$

Equation (2) is similar to eqn (14) derived by GREENLAND (1970).

The concentration in the solid assemblage crystallizing at given value of F , is calculated from:

$$C^S(F) = D(F)C^L(F) \quad (3)$$

Equation (3) is only valid in the absence of trapped intercumulus liquid.

The leuconoritic adcumulates and charnockitic residual liquids

Although these two rock types were formed after the anorthositic orthocumulates, they will be treated first, because: (i) without a trapped liquid as a complicating factor the leuconorites are easier to model; (ii) the fractionation history of late stage liquids needs to be known to understand the trace element characteristics of the anorthosite orthocumulates.

Our model (Fig. 7) quite successfully reproduces the observed REE patterns of the leuconoritic cumulates 249-1/1 and 334-1/1, and the least evolved charnockitic liquid 443-4/1. Taken at face value, the results imply that sample 249-1/1 formed very early in the leuconorite crystallization stage, while sample 334-1/1 corresponds to the solid precipitating at ca. 60% solidification. But it is equally plausible that the higher REE abundances of 334-1/1 merely reflect a higher abundance of apatite, as suggested by its higher P content (Table 1). Indeed, the 1% apatite assumed to be present in the leuconorites accounts for about 30% of their total REE inventory. This simple argument highlights the inherent difficulties of modelling cumulate rocks. Our calculations apparently fail to account

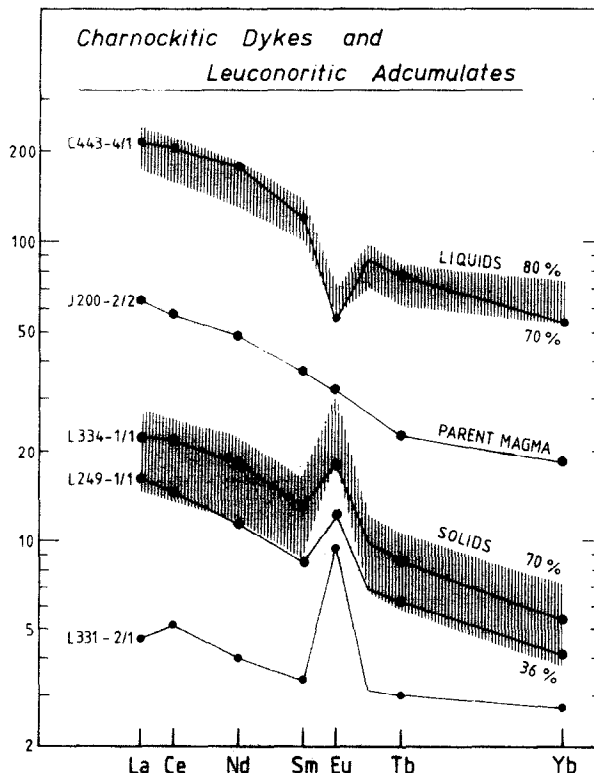


Fig. 7. Observed and calculated (dashed fields) chondrite-normalized REE patterns of the leuconoritic adcumulates and the charnockitic residual liquids, based on the assumption that they formed by fractional crystallization from a jotunitic parental magma. The pattern of leuconorite L331-2/1 is not matched that well, because the modal composition of this sample differs considerably (higher orthopyroxene/plagioclase ratio and lower apatite) from the average composition adopted in the calculations.

for the REE distribution of leuconorite 331-2/1. Again, this may be largely due to the low apatite content of the sample: for the 0.05% P (Table 1) implies less than the 1%, modal apatite assumed in the calculations.

The Eu-anomalies of 249-1/1 and 334-1/1 are not matched that well. We assumed that the plagioclase Eu partition coefficient varied linearly as $K = 0.5 + 0.5F$. It seems that an exponential dependence on F would be more appropriate, with K increasing rather slowly during the first 50% solidification, followed by a steep rise to $K \geq 1$ in the later stages. Since the Eu partition coefficient will mainly depend on the ill-defined evolution of the oxygen fugacity, further refinements of the model are not deemed warranted.

We stressed earlier that the proportion of charnockites is difficult to estimate from field observations. Our model gives an estimate of about 25% charnockite (+ pegmatite) by mass, which is similar to an independent estimate based on a K-Rb evolution model (DUCHESNE and DEMAFFE, 1978).

We have not attempted to model the differentiation process in the charnockite stage ($F \geq 80\%$). It is expected that the REE fractionation will be more and more controlled by a residual fluid phase and by pre-

cipitation of accessory minerals (e.g. PETERSEN, 1980). The REE patterns of the three charnockites (Fig. 4) show that zircon and other phases concentrating the heavy REE played a very important role, as the La/Yb_N ratio increases from 4.1 to 15 and Yb decreases from 50 to 20 times the chondritic value. Our lack of knowledge of the appropriate partition coefficients and their compositional and temperature dependence (MYSEN and VIRGO, 1980) precludes any sound modelling.

The anorthositic orthocumulates

The REE pattern of sample 335-1/1 is consistent with very early crystallization from the jotunitic parental magma and virtually no trapped intercumulus liquid. However, the trapped liquid component completely dominates the trace element characteristics of samples 058-1/1 and 299-1/1 (Fig. 8).

The most remarkable aspect of samples 058-1/1 and 299-1/1 is that their trapped liquid must have been considerably more fractionated than the jotunitic magmas from which the plagioclase and orthopyroxene originally crystallized. This is strikingly illustrated by sample 299-1/1, that has even higher REE and Rb abundances than the proposed parental magma.

The overall composition of an orthocumulate rock

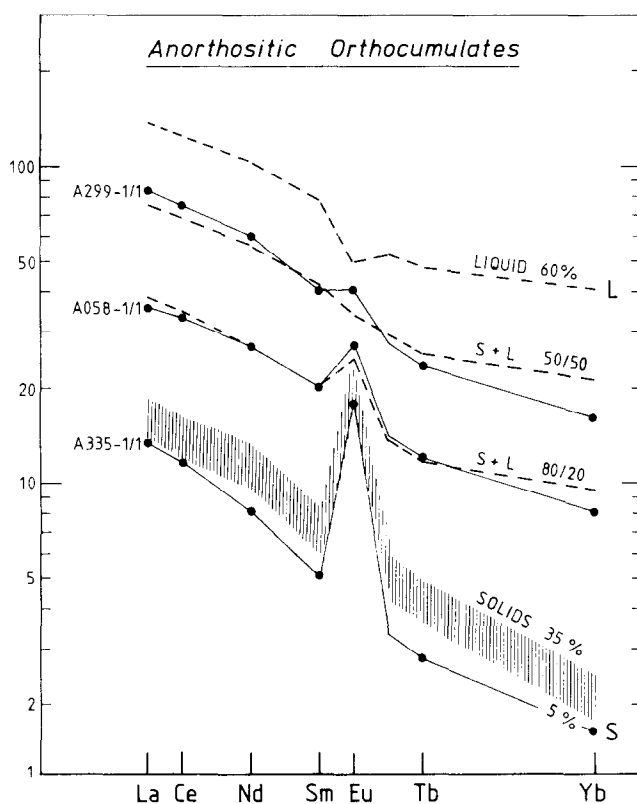


Fig. 8. The REE pattern of anorthosite A335-1/1 is consistent with very early crystallization from the jotunitic parental magma, with virtually no trapped intercumulus liquid present. The apparently highly fractionated intercumulus liquid dominates the REE characteristics of samples A058-1/1 and A299-1/1. The REE patterns can be matched rather well by mixtures of early cumulates ($S = A335-1/1$) and a differentiated liquid (L). The choice of residual liquid L , formed at 60% crystallization, is by no means unique: other combinations may give equally satisfactory matches.

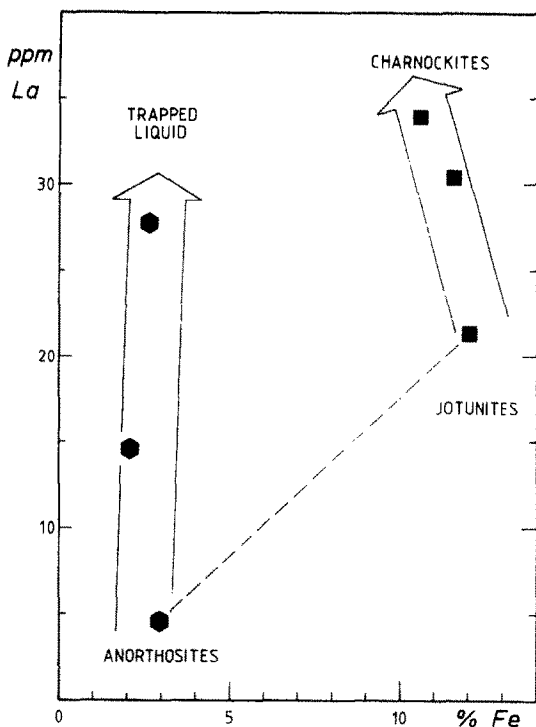


Fig. 9. The overall composition of an orthocumulate rock should lie on a mixing line connecting the original cumulate minerals and the trapped liquid. It is clear that the intercumulus liquid in the anorthosites must have been considerably more fractionated than the jotunitic parental magma from which the anorthosite originally crystallized. Compositional trends in the three anorthosites point to an intercumulus liquid with the characteristics of the charnockites, that are considered as late stage residual liquids formed from the jotunitic parental magma (charnockites plot off scale, having 3.5–6% total Fe and 72–108 ppm La; Tables 1–3). The same conclusions follow from similar figures using other element combinations.

should lie on a mixing line connecting the original cumulate minerals and the trapped liquid. Figure 9 was chosen as an example to show that samples 058-1/1 and 299-1/1 cannot possibly be considered as mixtures of a pure anorthosite adcumulate, such as 335-1/1, and a jotunitic liquid. Instead, Fig. 9 suggests that the intercumulus liquids at final solidification are similar—though not necessarily identical—to evolved charnockitic liquids. The same conclusion follows from other diagrams, using Rb, Sc, Co, etc.

Figure 8 illustrates that the REE patterns of 058-1/1 and 299-1/1 can be reproduced rather well by combinations of early anorthositic adcumulates (S) and a strongly fractionated liquid (L). The choice of residual liquid L, formed at 60% solidification, is by no means unique. Other combinations may give equally satisfactory matches. A more differentiated liquid would obviously require less trapped liquid, but up to 50% intercumulus liquid cannot be considered as unrealistically high (CAMPBELL *et al.*, 1978).

MAJOR ELEMENT CONSTRAINTS

Our model successfully reproduces the REE geo-

chemistry of the Hydra body, and is consistent with field relationships and petrographical observations. However, we recognize that REE modelling alone cannot be conclusive, since trace element fractionation calculations are to a large extent decoupled from the major element chemistry. Indeed, a hypothetical gabbroic anorthositic parent magma with similar REE abundances as the border jotunitites would be equally satisfactory in terms of REE.

The major element variation trends are unfortunately much more difficult to model in detail: nonetheless a simple argument based on mass balance considerations turned out to be quite instructive. Since we assumed that all the petrologically different components of the fractionation sequence are exposed in the Hydra body, an appropriately weighted sum of the major elements of the anorthosites, leuconorites and charnockites should add up to the composition of the jotunitic parent magma (assuming closed system fractionation). Table 6 summarizes the results of such a mass balance calculation for major and selected trace elements. Column S1 is the sum of anorthosites (average of samples 335-1/1, 058-1/1 and 299-1/1), leuconorites (average of 334-1/1 and 249-1/1) and charnockites (average of 443-4/1 and 283-2/2), using weighting factors of 0.35, 0.45 and 0.20 respectively (in accordance with the REE model). Composition S1 obviously differs considerably from the assumed jotunitic parental magma (J = jotunitite 200-2/2), as shown by the concentration ratios S1/J. Composition S1 is too rich in a plagioclase component (Sr, Al, Ca) and highly incompatible lithophile trace elements (Rb, Th), but too poor in a mafic component and associated trace elements (Ti, Fe³⁺, Fe²⁺, Mg, Sc, Co). Taken at face value, this calculation could be regarded as an argument in favor of a gabbroic anorthositic parental magma. However, we argued above that the occurrence of the jotunitites is difficult

Table 6.

Mass balance calculations for the Hydra Massif. (% for major elements; ppm for traces)

	J	S1	S2	S1/J	S2/J
SiO ₂	49.0	53.5	49.6	1.09	1.01
TiO ₂	4.5	2.3	4.1	0.51	0.91
Al ₂ O ₃	12.5	18.0	14.3	1.44	1.14
Fe ₂ O ₃	4.7	3.2	5.1	0.67	1.09
FeO	12.5	6.4	10.1	0.52	0.81
MgO	6.04	4.33	6.8	0.72	1.13
CaO	6.08	6.94	5.92	1.14	0.97
Na ₂ O	3.26	3.60	2.83	1.10	0.87
K ₂ O	1.33	1.60	1.20	1.20	0.90
P ₂ O ₅	0.40	0.16	0.15	0.40	0.38
Sc	25.9	13.6	18.9	0.53	0.73
Co	47.	39.	52.	0.83	1.11
Rb	22.6	38.	28.	1.68	1.24
Sr	372.	523.	409.	1.41	1.10
La	21.3	22.8	17.1	1.07	0.80
Yb	3.6	2.7	2.2	0.76	0.62
Th	1.2	1.9	1.5	1.57	1.24

J = jotunitite 200-2/2.

S1 and S2 = weighted sums of anorthosites, leuconorites, charnockites, and, for S2 only, of pyroxenites (see text for discussion).

to reconcile with a gabbroic anorthosite parental magma: it might hence be advantageous to consider alternative explanations for the apparent mass balance discrepancy.

Because field observations do not provide quantitative constraints, we neglected so far any fractionation of pyroxenes plus oxides from plagioclase due to differential crystal settling rates. But the sporadic occurrence of pyroxenitic masses in the leuconorites shows that this fractionation process actually played a role during solidification of the Hidra intrusion. It is quite conceivable that the exposed levels of the Hidra Massif are not entirely representative for the intrusion as a whole. Given the density differences between plagioclase and iron-bearing minerals, it looks plausible that the deeper zones of the intrusion are progressively enriched in heavy minerals, while the upper parts are enriched in plagioclase and charnockitic residual liquids. Column S2 in Table 6 accommodates such changes in the relative proportions of the various petrological components, using weighting factors of 0.20, 0.45, 0.15 and 0.20 for anorthosites, leuconorites, charnockites and pyroxenites (sample 328-2/1) respectively. Composition S2 is indeed a much better fit to the jotunitites than composition S1 (compare columns S1/J and S2/J).

The required changes in the fractionation model of the Hidra Massif do not basically affect the REE model outlined above. Since orthopyroxene and Fe, Ti-oxides do not appreciably fractionate the REE, a larger proportion can only enhance the absolute REE contents in the liquid by at maximum 30% at any stage of the crystallization process.

DISCUSSION

Role of plagioclase flotation?

The inference that plagioclase crystals are enriched relative to mafic phases in the exposed upper part of the Hidra intrusive body, suggests that plagioclase might have had a tendency to float in the jotunitic parental magma. Calculations based on the partial molar volumes from BOTTINGA and WEILL (1970) give a density of $2.67 \text{ g}\cdot\text{cm}^{-3}$ (at 1200°C and 1 kbar pressure) for a liquid with the composition of jotunitite J200-2.2. The main uncertainties in the density estimates are the H_2O content and $\text{Fe}^{3+}/\text{Fe}^{2+}$ ratio of the magma. A decrease of the $\text{Fe}^{3+}/\text{Fe}^{2+}$ ratio raises the density of the liquid, while an increase of the H_2O content lowers the density ($2.64 \text{ g}\cdot\text{cm}^{-3}$ for 1% H_2O at 1200°C and 1 kbar). Despite these uncertainties, it appears quite plausible that the jotunitic magmas had a significantly higher density than the early crystallizing An_{55-45} plagioclase crystals (density of $2.63 \pm 0.01 \text{ g}\cdot\text{cm}^{-3}$ at 1200°C ; CAMPBELL *et al.*, 1978). And if Campbell *et al.* are correct, the floating tendency of plagioclase might actually be $0.03 \text{ g}\cdot\text{cm}^{-3}$ greater than indicated by liquid density calculations.

The apparent underabundance of mafic phases in the exposed levels and the likelihood of plagioclase

flotation could imply that plagioclase was a less abundant liquidus phase in the initial stages of crystallization than suggested by the modal composition of the anorthosites (plagioclase/mafic $\cong 82/17$). It is conceivable that the transition from the 'anorthositic' to 'leuconoritic' crystallization stage mainly marks a reversal of plagioclase flotation to plagioclase sinking, due to the decreasing density of the residual liquids. The rising H_2O content of the liquid is a fairly critical parameter in this respect (see e.g. Fig. 7 of CAMPBELL *et al.*, 1978).

As an alternative to plagioclase flotation, one could invoke a flowage differentiation process (BHATTACHARJI and SMITH, 1964) to explain the enrichment of early formed plagioclase crystals and their association with a highly differentiated intercumulus liquid in the axial zone of the Hidra Massif. Indeed, EMSLIE (1965) and BUDDINGTON (1969) suggested this fractionation process for some anorthositic series. However, the chilled margin of an intrusion that fractionates via flowage differentiation is more likely a residual liquid rather than a parental magma. But the Hidra jotunitites can hardly be regarded as residual magmas. Firstly, they lack the negative Eu-anomalies expected for liquids formed after precipitation of large amounts of plagioclase. Secondly, the locally contain plagioclase phenocrysts of nearly the same composition (An_{45-50}) as the large plagioclases (An_{48-55}) from the axial anorthosites. The latter observation actually seems to rule out that flowage differentiation played a major role in the evolution of the Hidra Massif.

The comagmatic character of the anorthosites and charnockites

The weighted average abundances of REE and other incompatible trace elements in plagioclase rich cumulate rocks of anorthositic massifs are lower than in any conceivable parental magma. By necessity, there must be a residual liquid rich in incompatible elements. The charnockites and pegmatites are the prime candidates in the Hidra Massif. Independent evidence for the silicic nature of the residual liquid of the Hidra fractionation can be inferred from the composition of the trapped intercumulus liquid in the anorthositic orthocumulates. We showed earlier (Fig. 9) that the intercumulus liquid must be fairly similar to the charnockites. This similarity is not limited to the REE and other incompatible lithophile elements; the compositional trends (Tables 1-3) defined by samples 335-1/1, 058-1/1 and 299-1/1 imply that the intercumulus liquid had the rather low Ti, Fe, Mg, Ca and Sr contents typical for the charnockites. Strictly speaking, these observations do not present unequivocal evidence for a comagmatic character of the Hidra anorthositic rocks and the charnockites. But it shows that the Hidra fractionation did not lead to mafic, Fe, Ti-rich late stage differentiates, as suggested by ASHWAL and SEIFERT (1980) in their study of the Adirondacks anorthosites. Besides, mafic dykes have not been observed in the Hidra Massif.

Obviously, the higher initial strontium isotopic ratios of the charnockites (Table 2) could be taken as strong evidence against a comagmatic character of anorthosites and charnockites. To circumvent this problem, one has to assume that the charnockitic liquids have been contaminated with supracrustal material. But this may not be an implausible assumption. Since the mass of charnockitic liquids was relatively small, they might have been particularly prone to contamination with fluids or low-melting liquids released from the gneissic envelope (having $^{87}\text{Sr}/^{86}\text{Sr} = 0.720\text{--}0.725$ at the time of the Hydra intrusion; VERSTEEVE, 1975). We therefore feel that the overall evidence (field relationships, trace element mass balance) is in favor of a comagmatic character of the Hydra anorthosites and charnockites.

CONCLUSIONS

The petrographical and geochemical evolution of the Hydra Massif is consistent with fractional crystallization of mainly plagioclase and orthopyroxene from a jotunitic (monzodioritic) magma. The parental magma occurs as a fine-grained border facies.

Partitioning into the cumulate minerals governs the trace element contents of the leuconoritic accumulates. On the contrary, the trace element characteristics of many anorthositic orthocumulates largely depends upon the trapped intercumulus liquid. This trapped liquid appears much more fractionated than the parental magmas from which the anorthite-rich plagioclase crystals originally crystallized.

The residual magma of the Hydra fractionation is represented by charnockitic dykes and pegmatitic lenses. The higher initial $^{87}\text{Sr}/^{86}\text{Sr}$ ratios of the charnockites point to contamination by surrounding gneissic material.

Major element mass balance constraints indicate that mafic phases are underabundant in the exposed levels of the Hydra Massif. It is conceivable that this reflects plagioclase flotation in the early stages of solidification.

Acknowledgements—This work has been carried out when both authors were research assistants of the National Fund for Scientific Research (Belgium). We are grateful to E. B. WATSON, S. S. STROMM and an anonymous referee for constructive reviews.

REFERENCES

- ADAMSON O. J. (1942) The granite pegmatites of Hitterø, SW Norway. *Geol. Foeren. Stockholm Foerh.* **64**, 97–116.
- ALBAREDE F. and BOTTINGA Y. (1972) Kinetic disequilibrium in trace element partitioning between phenocrysts and host lava. *Geochim. Cosmochim. Acta* **36**, 141–156.
- ANDERSON A. T. and MORIN M. (1969) Two types of massif anorthosites and their implications regarding the thermal history of the crust. In *Origin of Anorthosites and Related Rocks* (ed. Y. W. Isachsen) *N.Y. State Mus. Sci. Serv. Mem.* **18**, 57–69.
- ASHWAL L. D. and SEIFERT K. E. (1980) Rare-earth-element geochemistry of anorthosite and related rocks from the Adirondacks, New York. *Geol. Soc. Am. Bull. Part II* **91**, 659–684.
- BHATTACHARJI S. and SMITH C. H. (1964) Flowage differentiation. *Science* **145**, 150–153.
- BOTTINGA Y. and WEILL D. F. (1970) Densities of liquid silicate systems calculated from partial molar volumes of oxide components. *Am. J. Sci.* **269**, 169–182.
- BUDDINGTON A. F. (1969) Adirondacks anorthosite series. In *Origin of Anorthosites and Related Rocks* (ed. Y. W. Isachsen). *N.Y. State Mus. Sci. Serv. Mem.* **18**, 215–232.
- CAMPBELL I. H., ROEDER P. L. and DIXON J. M. (1978) Plagioclase buoyancy in basaltic liquids as determined with a centrifuge furnace. *Contrib. Mineral. Petrol.* **67**, 369–377.
- CARMICHAEL I. S. E., TURNER F. J. and VERHOOGEN J. (1974) *Igneous Petrology*. McGraw-Hill.
- DEMAÏFFE D. (1977a) De l'origine des anorthosites. *Pétrologie, Géochimie et Géochimie isotopique des massifs anorthositiques d'Hydra et de Garsaknatt*. Ph.D. dissertation, Univ. Libre de Bruxelles.
- DEMAÏFFE D. (1977b) Les massifs satellites anorthosito-leuconoritiques d'Hydra et de Garsaknatt: leur signification pétrogénétique. *Ann. Soc. Géol. Belg.* **100**, 167–174.
- DEMAÏFFE D. and JAVOY M. (1980) $^{18}\text{O}/^{16}\text{O}$ Ratios of anorthosites and related rocks from the Rogaland Complex (S.W. Norway). *Contrib. Mineral. Petrol.* **72**, 311–317.
- DEMAÏFFE D., DUCHESNE J. C., MICHOT J. and PASTEELS P. (1973) Le massif anorthosito-leuconoritique d'Hydra et son faciès de bordure. *C.R. Acad. Sci. Ser. D* **277**, 17–20.
- DEMAÏFFE D., MICHOT J. and PASTEELS P. (1974) Time relationship and Sr isotopic evolution in the magma of the anorthosite-charnockite suite of S. Norway. *Int. Meet. for Geochronology, Cosmochronology and Isotope Geology*, Paris (Abstract).
- DEMAÏFFE D., DUCHESNE J. C. and HERTOGEN J. (1979) Trace element variations and isotopic composition of charnockitic acidic rocks related to anorthosites (Rogaland-S.W. Norway). In *Origin and Distribution of the Elements, 2nd Symp.* (ed. L. H. Ahrens), pp. 417–429. Pergamon Press.
- DE WAARD D., DUCHESNE J. C. and MICHOT J. (1974) Anorthosites and their environment. In *Géologie des Domaines Cristallins, Centenaire Soc. Géol. Belg.* Liège, pp. 323–346.
- DRAKE M. J. (1972) The distribution of major and trace elements between plagioclase feldspar and magmatic silicate liquid: an experimental study. Ph.D. dissertation, Univ. of Oregon.
- DRAKE M. J. and WEILL D. F. (1975) Partition of Sr, Ba, Ca, Y, Eu^{2+} , Eu^{3+} and other REE between plagioclase feldspar and magmatic liquid: an experimental study. *Geochim. Cosmochim. Acta* **39**, 689–712.
- DUCHESNE J. C. (1972) Iron-titanium oxide minerals in the Bjerkrem-Sogndal massif. *J. Petrol.* **13**, 57–81.
- DUCHESNE J. C. (1978) Quantitative modelling of Sr, Ca, Rb and K in the Bjerkrem-Sogndal layered lopolith (S.W. Norway). *Contrib. Mineral. Petrol.* **66**, 175–184.
- DUCHESNE J. C. and DEMAÏFFE D. (1978) Trace elements and anorthosite genesis. *Earth Planet. Sci. Lett.* **38**, 249–272.
- DUCHESNE J. C., ROELANDTS I., DEMAÏFFE D., HERTOGEN J., GIJBELS R. and DE WINTER J. (1974) REE data on monzonitic rocks related to anorthosites and their bearing on the nature of the parental magma of the anorthosite series. *Earth Planet. Sci. Lett.* **24**, 325–335.
- EMSLIE R. F. (1965) The Michikamau anorthositic intrusion, Labrador. *Can. J. Earth Sci.* **2**, 385–399.
- EMSLIE R. F. (1978) Anorthosite massifs, rapakivi granites, and late Proterozoic rifting of North America. *Precambrian Res.* **7**, 61–98.
- GREEN T. H., BRUNFELT A. O. and HEIER K. S. (1972) Rare-earth element distribution and K/Rb ratios in granulites.

- mangerites and anorthosites, Lofoten-Vesteraalen, Norway. *Geochim. Cosmochim. Acta* **36**, 241–257.
- GREENLAND L. P. (1970) An equation for trace element distribution during magmatic crystallization. *Am. Mineral.* **55**, 455–465.
- GRIFFIN W. L., SUNDVOLL F. and KRISTMANNOTTIR H. (1974) Trace element composition of anorthosite plagioclase. *Earth Planet. Sci. Lett.* **24**, 213–223.
- GRUTZECK M. W., KRIDELBAUGH S. J. and WEILL D. F. (1974) The distribution of Sr and the REE between diopside and silicate liquid. *Geophys. Res. Lett.* **1**, 273–275.
- HENDERSON P. and WILLIAMS C. T. (1979) Variation in trace element partition (crystal/magma) as a function of crystal growth rate. In *Origin and Distribution of the Elements, 2nd Symp.* (ed. L. H. Ahrens), pp. 191–198. Pergamon Press.
- HENDERSON P., FISHLOCK S. J., LAUL J. C., COOPER T. D., CONARD R. L., BOYNTON W. V. and SCHMITT R. A. (1976) Rare earth element abundances in rocks and minerals from the Fiskenaesset Complex, West Greenland. *Earth Planet. Sci. Lett.* **30**, 37–49.
- HERTOGEN J. and GIJBELS R. (1971) Instrumental neutron activation analysis of rocks with a low-energy photon detector. *Anal. Chim. Acta* **56**, 61–82.
- IRVING A. J. (1978) A review of experimental studies of crystal/liquid trace element partitioning. *Geochim. Cosmochim. Acta* **42**, 743–770.
- KUDO A. M. and WEILL D. F. (1970) An igneous plagioclase thermometer. *Contrib. Mineral. Petrol.* **25**, 52–65.
- McKAY G. A. and WEILL D. F. (1976) Petrogenesis of KREEP. *Proc. 7th Lunar Planet. Sci. Conf.*, Houston, Vol. 2, pp. 2427–2447. Pergamon Press.
- MICHOT P. (1960) La géologie de la catazone: le problème des anorthosites, la palingénèse basique et la tectonique catazonale dans le Rogaland méridional. *Norges Geol. Unders.* **212**, 1–54.
- MICHOT J. and MICHOT P. (1969) The problem of anorthosites: the South Rogaland Complex, S.W. Norway. In *Origin of Anorthosites and Related Rocks* (ed. Y. W. Isachsen). *N.Y. State Mus. Sci. Serv. Mem.* **18**, 399–410.
- MURTHY V. R. and GRIFFIN W. L. (1969) K/Rb fractionation by plagioclase feldspars. *Chem. Geol.* **6**, 262–271.
- MYSEN B. O. and VIRGO D. (1980) Trace element partitioning and melt structure: an experimental study at 1 atm pressure. *Geochim. Cosmochim. Acta* **44**, 1917–1930.
- NAGASAWA H. (1970) Rare earth concentrations in zircons and apatites and their host dacites and granites. *Earth Planet. Sci. Lett.* **9**, 359–364.
- PASTEELS P. and MICHOT J. (1975) Geochronologic investigation of the metamorphic terrain of S.W. Norway. *Norsk Geol. Tidssk.* **55**, 111–134.
- PASTEELS P., DEMAÏFFE D. and MICHOT J. (1979) U–Pb and Rb–Sr geochronology of the eastern part of the south Rogaland igneous complex, southern Norway. *Lithos* **12**, 199–208.
- PETERSEN J. S. (1980) Rare-Earth element fractionation and petrogenetic modelling in charnockitic rocks. Southwest Norway. *Contrib. Mineral. Petrol.* **73**, 161–172.
- PHILPOTTS A. R. (1969) Parental magma of the anorthosite–mangerite suite. In *Origin of Anorthosites and Related Rocks* (ed. Y. W. Isachsen) *N.Y. State Mus. Sci. Serv. Mem.* **18**, 207–212.
- PHILPOTTS A. R. (1978) Liquid immiscibility in anorthosite–quartz mangerite series. *Abstr. Joint Ann. Meet. GAC-MAC-GSA*, Toronto, pp. 471–472.
- PHILPOTTS J. A., SCHNETZLER C. C. and THOMAS H. H. (1966) REE abundances in an anorthosite and a mangerite. *Nature* **212**, 805–806.
- RYERSON F. J. and HESS P. C. (1978) Implications of liquid–liquid distribution coefficients to mineral–liquid partitioning. *Geochim. Cosmochim. Acta* **42**, 921–932.
- SCHNETZLER C. C. and PHILPOTTS J. A. (1970) Partition coefficients of rare-earth elements between igneous matrix material and rock-forming mineral phenocrysts. II. *Geochim. Cosmochim. Acta* **34**, 331–340.
- SCHOCK H. H. (1979) Distribution of Rare-earth and other trace elements in magnetites. *Chem. Geol.* **26**, 119–133.
- SIMMONS E. G. and HANSON G. N. (1978) Geochemistry and origin of massif-type anorthosites. *Contrib. Mineral. Petrol.* **66**, 119–135.
- SIMMONS E. G., HANSON G. N. and LUMBERS S. B. (1980) Geochemistry of the Shawmere anorthositic complex, Kapuskasing structural zone, Ontario. *Precambrian Res.* **11**, 43–71.
- VERSTEEVE A. (1975) Isotope geochronology of the high-grade metamorphic Precambrian of Southwestern Norway. *Norges Geol. Unders.* **318**, 1–50.
- WATSON E. B. (1976) Two-liquid partition coefficients: experimental data and geochemical implications. *Contrib. Mineral. Petrol.* **56**, 119–134.
- WATSON E. B. (1980) Some experimentally determined zircon/liquid partition coefficients for the rare earth elements. *Geochim. Cosmochim. Acta* **44**, 895–897.
- WEILL D. F. and McKAY G. A. (1975) The partitioning of Mg, Fe, Sr, Ce, Sm, Eu, and Yb in lunar igneous systems and a possible origin of KREEP by equilibrium partial melting. *Proc. 6th Lunar Planet. Sci. Conf.*, Houston, Vol. 1, pp. 1143–1158. Pergamon Press.
- WIEBE R. A. (1979) Fractionation and liquid immiscibility in an anorthositic pluton of the Nain Complex, Labrador. *J. Petrol.* **20**, 239–269.
- WIEBE R. A. (1980) Anorthositic magmas and the origin of proterozoic anorthosite massifs. *Nature* **286**, 564–567.